PHYSICAL REVIEW A **90**, 062706 (2014)

Time-dependent calculations of transfer ionization by fast proton-helium collision in one-dimensional kinematics

Vladislav V. Serov
Department of Theoretical Physics, Saratov State University, 83 Astrakhanskaya, Saratov 410012, Russia

A. S. Kheifets
Research School of Physical Sciences, The Australian National University, Canberra ACT 2601, Australia
(Received 29 October 2014; published 8 December 2014)

We analyze a transfer ionization (TI) reaction in the fast proton-helium collision $H^+ + He \to H^0 + He^{2+} + e^-$ by solving a time-dependent Schrödinger equation (TDSE) under the classical projectile motion approximation in one-dimensional kinematics. In addition, we construct various time-independent analogs of our model using lowest-order perturbation theory in the form of the Born series. By comparing various aspects of the TDSE and the Born series calculations, we conclude that the recent discrepancies of experimental and theoretical data may be attributed to deficiency of the Born models used by other authors. We demonstrate that the correct Born series for TI should include the momentum-space overlap between the double-ionization amplitude and the wave function of the transferred electron.

DOI: 10.1103/PhysRevA.90.062706 PACS number(s): 34.70.+e, 34.10.+x, 34.50.Fa

I. INTRODUCTION

The transfer ionization (TI) reaction in a fast proton-helium collision $H^+ + He \to H^0 + He^{2+} + e^-$ has been studied thoroughly, both experimentally and theoretically, over several decades. The initial studies have been performed by coincident detection of various reaction fragments [1,2]. The first systematic observation of the fully differential momentum distribution of the ejected electron [3] revealed the potential of this reaction to examine radial and angular correlations in the helium-atom ground state. This potential was further explored in Refs. [4,5]. Several reaction mechanisms were identified by studying the recoil-ion momentum distribution [6]. Later on, the experimental setup was improved to detect the complete three-particle coincidence $H - He^{2+} - e^-$ and to map three-dimensional ejected electron momentum distributions [7–9]. Along with proton-helium collisions, heavier ions were also used as projectiles [10,11].

On the theoretical side, various calculations were performed employing the lowest-order perturbation theory in the form of the Born series. The initial first Born results [9,12] confirmed that the fully differential cross sections for TI were indeed a sensitive probe of the ground-state correlation in the helium-atom ground state. By employing ground-state wave functions of various levels of sophistication, better or worse agreement with the experiment could be achieved. A more detailed comparison with experimental data, in the form of the fully differential cross sections, was not possible at the time. Indeed, in the earlier experiments [3,4], the momentum distribution of the ionized electron was derived from the momentum and energy conservation with other collision partners, but not directly measured as in the latest experiments [7,8]. Nevertheless, the authors of Ref. [12] continued their quest and included the second Born corrections into their model in the form of the closure term [13]. Improvement to the first Born results was marginal in terms of their agreement with the experimental data.

A similar first Born model of another group of authors [14] was used to interpret three-dimensional electron-momentum distributions in a series of joint experimental and theoretical works [7,8]. Similarly to the initial studies by Godunov *et al.* [9,12,13], a strong sensitivity of the calculated results was demonstrated to the quality of the helium-atom ground-state wave function. However, agreement with the experimental data was qualitative at best. It was hoped that extension of the theoretical model to the second Born treatment would have improved this agreement. However, such an extension reported earlier [13] was not very efficient. General utility of the second Born corrections is discussed in Ref. [15].

In their perturbative treatment, both groups of authors identified three terms in the first Born amplitude of the TI reaction. These terms can be associated with various terms of the interaction potential $V_{p1} + V_{p2} + V_{Np}$ when this amplitude is expressed in its *prior* form. This potential describes the interaction of the projectile proton with the two target electrons and the nucleus.

The first term, associated with V_{p1} and denoted by A_1 in Refs.[7,8,14] or termed "transfer first" in Refs. [9,12,13], is shown to be identical to the Oppenheimer, Brinkmann, and Kramers (OBK) amplitude and describes the collision between the target electron labeled 1 and the proton followed by the capture of this electron by the projectile. The second electron, labeled 2, is released due to rearrangement in the helium atom, known as the shakeoff (SO) process. In principle, in the $e - H^+$ interaction can be factored out from the OBK term A_1 [7]. The remaining SO amplitude provides a simplified theoretical treatment of TI that was applied in Refs. [4,5]. The second term, associated with V_{p2} and denoted by A_2 or termed as "ionization first," describes the process in which the proton knocks off a target electron 1 into the continuum, followed by capturing the remaining electron 2 from the helium atom. The third term, associated with V_{pN} and denoted by A_3 represents an initial interaction between the projectile and the helium nucleus followed by the electron capture. Similarly to A_1, the second electron is also released due to the sudden rearrangement in the helium ion.

Unlike the other authors, Voitkiv *et al.* [16–18] expressed the first Born amplitude in the *post* form which contained a

different interaction potential $V_{N1} + V_{p2} + V_{12} + V_{Np}$. They identified an additional electron-electron Auger mechanism of TI associated with the term V_{12}. In this mechanism, the electron to be transferred rids itself of the excess energy not via the coupling to the radiation field, as in the radiative capture process, but by interaction with the other electron. Inclusion of this mechanism improved significantly agreement with experimental data [10] even though some quantitative discrepancies remained. In their comment on Voitkiv and Ma [18], Popov *et al.* [19] argued that since both the *prior* and *post* forms of the first Born amplitude should be identical, the newly discovered electron-electron Auger mechanism was, in fact, contained in the long-known OBK amplitude. In their reply, Voitkiv and Ma [20] retorted this argument by pointing to the shortcomings of the OBK approximation.

Outside the first Born treatment lies the process of repeated interaction of the projectile with the target in which both the target electrons are ejected in sequence. This sequential process is known in the electron-impact ionization and double photoionization as the two-step-2 process [21]. For the purpose of this study we will call it binary encounter (BE). The signatures of the SO and BE processes in TI can be found in the momentum distribution of the ejected electron. In the BE process, the ejected electron flies predominantly in the forward direction (in the direction of the projectile), due to the momentum transferred from the projectile. In the SO process, the emitted electron flies predominantly backwards because the instantaneous momenta of an electron pair in the helium-atom ground state are aligned in the opposite directions. The SO process is contained in the first Born amplitude while the BE process can be only accommodated by further terms in the Born series. At small velocities of the projectile, the BE mechanism dominates, whereas at large velocities it is the SO mechanism that becomes dominant.

When the Born series calculations cannot reproduce the experimental data on a quantitative level, an additional insight into the TI reaction can be gained by a nonperturbative approach based on solving the time-dependent Schrödinger equation (TDSE). For a four-body Coulomb problem such as TI, the TDSE cannot be solved in its full dimensionality and additional approximations should be made. In the experiments [3,7,8], the projectile proton had the velocity $v_p \simeq 5$ a.u. and the momentum $p_p \simeq 10^4$ a.u. This corresponds to the wavelength $\lambda_p \sim 10^{-3}$ a.u. which is much less than the atom size. Due to this fact and because of a small relative change of the projectile velocity, the classical projectile motion approximation (CPA) should be sufficiently accurate. The TI reaction in this approximation is described by a six-dimensional TDSE which can be solved, in principle, using modern computational facilities. Nevertheless, for the purpose of this work, we further simplify the problem and restrict the motion of all the particles to one dimension (1D). We compare results of thus restricted TDSE calculation with various perturbative Born calculations, also reduced to 1D. By analyzing various aspects of the TDSE and the Born series calculations, we conclude that the recent discrepancies of experimental and theoretical data may be explained by deficiency of theoretical approach used by other authors. We demonstrate that the correct Born series for TI should include the momentum-space overlap between the ionization amplitude and the wave function of the transferred electron.

II. THEORETICAL MODEL

Within the scope of the CPA, the full-dimensional TDSE takes the form

$$i\frac{\partial\Psi(\mathbf{r}_1,\mathbf{r}_2,t)}{\partial t} = \left[\hat{H}_0 - \frac{1}{|\mathbf{r}_1-\mathbf{R}(t)|} - \frac{1}{|\mathbf{r}_2-\mathbf{R}(t)|}\right]\Psi(\mathbf{r}_1,\mathbf{r}_2,t), \quad (1)$$

with the initial condition

$$\Psi(\mathbf{r}_1,\mathbf{r}_2,t_0) = \Phi_0(\mathbf{r}_1,\mathbf{r}_2)\exp(-iE_0t_0); \quad t_0 \to -\infty. \quad (2)$$

Here, $\mathbf{R}(t) = (b,0,v_pt)$ is a current position of a proton, b is an impact parameter, $\Phi_0(\mathbf{r}_1,\mathbf{r}_2)$ is the target ground-state function, and $\hat{H}_0$ is target Hamiltonian, which for the helium atom has the form

$$\hat{H}_0 = -\frac{1}{2}\nabla_1^2 - \frac{1}{2}\nabla_2^2 - \frac{1}{r_1} - \frac{1}{r_2} + \frac{1}{|\mathbf{r}_2-\mathbf{r}_1|}. \quad (3)$$

For a one-dimensional kinematics, Eq. (1) is reduced to two-dimensional TDSE

$$i\frac{\partial\psi(x_1,x_2,t)}{\partial t} = [\hat{H}_0 + U_1(x_1-v_pt) + U_1(x_2-v_pt)]\psi(x_1,x_2,t) \quad (4)$$

with the initial condition

$$\psi(x_1,x_2,t_0) = \varphi_0(x_1,x_2)\exp(-iE_0t_0); \quad t_0 \to -\infty \quad (5)$$

and the Hamiltonian

$$\hat{H}_0 = -\frac{1}{2}\frac{\partial^2}{\partial x_1^2} - \frac{1}{2}\frac{\partial^2}{\partial x_2^2} + U_2(x_1) + U_2(x_2) + U_{-1}(x_2-x_1). \quad (6)$$

Here, the effective potentials $U_Z(x \to \pm\infty) = -Z/|x|$ is taken in the form of a shifted Coulomb potential

$$U_Z(x) = -\frac{Z}{|x| + |Z|^{-1}}. \quad (7)$$

With this potential, the hydrogenlike ion is described by a 1D equation

$$\left[-\frac{1}{2}\frac{\partial^2}{\partial x^2} + U_Z(x)\right]\varphi_n^Z(x) = \epsilon_n^Z\varphi_n^Z(x) \quad (8)$$

with the ground-state energy $\epsilon_0^Z = -Z^2/2$ being equal to the ground-state energy of a conventional 3D ion. The ground-state wave function

$$\varphi_0^Z(x) = \sqrt{\frac{2Z}{5}}(1+Z|x|)\exp(-Z|x|), \quad (9)$$

when Fourier transformed to the momentum space

$$\varphi_0^Z(x) = \frac{1}{\sqrt{2\pi}}\int_{-\infty}^{\infty} u_0^Z(\varkappa)e^{i\varkappa x}d\varkappa \quad (10)$$

becomes

$$u_0^Z(p) = \frac{4}{\sqrt{5\pi Z}}\frac{1}{[1+(p/Z)^2]^2}. \quad (11)$$

This only differs by a normalization constant from a conventional ground-state wave function of a hydrogenlike ion in the momentum space

$$u_{100}(p) = \frac{2\sqrt{2}}{\pi Z^{3/2}} \frac{1}{[1+(p/Z)^2]^2} .$$

It is a useful property that allows one to maintain the correct dependence of the TI cross section on v_p which is determined by the momentum-space overlap. The Fourier transform of the potential (7)

$$V_Z(q) = \int_{-\infty}^{\infty} e^{-iq\xi} U_Z(\xi) d\xi = 2Z\left(\sin\left|\frac{q}{Z}\right| \mathrm{Ssi}\left|\frac{q}{Z}\right| + \cos\left|\frac{q}{Z}\right| \mathrm{Ci}\left|\frac{q}{Z}\right| \right) \quad (12)$$

can be expressed via the cosine integral $\mathrm{Ci}\,(x)$ and the shifted sine integral $\mathrm{Ssi}\,(x)$.

For better readability, in the text following we will use the notation $\epsilon_{\mathrm{H}} \equiv \epsilon_0^1$ for the hydrogen-atom energy, and $\varphi_{\mathrm{H}}(x) \equiv \varphi_0^1(x)$ and $u_{\mathrm{H}}(p) \equiv u_0^1(p)$ for the 1D hydrogen-atom ground-state wave function in coordinate and momentum space, respectively. The energy and ground-state wave function of 1D He^+ ion ($Z = 2$) are designated simply as $\epsilon_0 \equiv \epsilon_0^Z$, $\varphi_0(x) \equiv \varphi_0^Z(x)$, and $u(p) \equiv u_0^Z(p)$.

The wave function of the electron captured by the projectile is

$$\psi_{\mathrm{tr}}(x,t) = \varphi_{\mathrm{H}}(x - v_p t) \exp\left[i v_p x - i\left(\frac{v_p^2}{2} + \epsilon_{\mathrm{H}}\right) t \right]. \quad (13)$$

If the second electron is ejected with the momentum k, the two-electron wave function of the final state can be written as

$$\psi_{k\mathrm{H}}(x_1,x_2,t) = \frac{1}{\sqrt{2}}[\psi_{\mathrm{tr}}(x_1,t)\varphi_k^{(-)}(x_2) + \psi_{\mathrm{tr}}(x_2,t)\varphi_k^{(-)}(x_1)] e^{-i\frac{k^2}{2}t}, \quad (14)$$

where $\varphi_k^{(-)}(x)$ is the continuum state function for the ejected electron with the energy $\epsilon = k^2/2$ in the field of a nucleus with $Z = 2$. The amplitude of TI is given by the following expression:

$$A(k) = \lim_{t\to\infty} \int_{-\infty}^{\infty}\int_{-\infty}^{\infty} \psi_{k\mathrm{H}}^*(x_1,x_2,t)\psi(x_1,x_2,t) dx_1 dx_2. \quad (15)$$

In the 1D case, the role of differential cross section of TI is assumed by the probability density

$$P^{(1)}(k) = \frac{dP}{dk} = |A(k)|^2 . \quad (16)$$

Using the exchange symmetry of the two-electron wave function $\psi(x_2,x_1,t) = \psi(x_1,x_2,t)$, we can split the integration in Eq. (15) in two steps. First, we calculate the wave function of the second electron when the first electron is transferred

$$\chi(x_2,t) = \sqrt{2}\int_{-\infty}^{\infty} \psi_{\mathrm{tr}}^*(x_1,t)\psi(x_1,x_2,t) dx_2 . \quad (17)$$

Next, we calculate the amplitude of ejection of the second electron

$$A(k) = \lim_{t\to\infty} \int_{-\infty}^{\infty} \varphi_k^{(-)*}(x) \exp\left(i\frac{k^2}{2}t\right) \chi(x,t) dx . \quad (18)$$

In the second step, for extraction of the ionization amplitudes from $\chi(x_2,t)$, we used the E-SURFF method [22]. Equation (4) was solved numerically using the simplest three-point finite difference scheme for evaluation of the space derivatives, and the split-step method for the time evolution. The target ground-state function $\varphi_0(x_1,x_2)$ was calculated using the evolution in the imaginary time providing the ground-state energy $E_0 = -3.35$ a.u.

To compare the role of the SO and BE processes, we also performed calculations for the case of zero interelectron potential. In such a case, the SO is absent and only the BE contributes to TI. For that reason, we named this approximation BECPA. In this approximation, Eq. (4) can be split in two identical equations

$$i\frac{\partial\psi(x,t)}{\partial t} = [\hat{h}_0 + U_1(x - v_p t)]\psi(x,t) \quad (19)$$

with

$$\hat{h}_0 = -\frac{1}{2}\frac{\partial^2}{\partial x^2} + U_2(x) \quad (20)$$

and the initial condition

$$\psi(x,t_0) = \varphi_0(x) e^{-i\epsilon_0 t_0}; \quad t_0 \to -\infty. \quad (21)$$

The wave function of a nontransferred electron in this approximation is

$$\chi(x,t) = \sqrt{2} C_{\mathrm{tr}}[\psi(x,t) - C_{\mathrm{tr}}\psi_{\mathrm{tr}}(x,t)], \quad (22)$$

where the transfer amplitude is

$$C_{\mathrm{tr}} = \lim_{t\to\infty} \int_{-\infty}^{\infty} \psi_{\mathrm{tr}}^*(x,t)\psi(x,t) dx. \quad (23)$$

III. RESULTS AND DISCUSSION

The probability density $P^{(1)}(k)$ (16) as a function of the ejected electron momentum is shown in Fig. 1 for the three selected proton velocities $v_p = 3$ a.u. (top), 5 a.u. (middle), and 10 a.u. (bottom). Results of the full CPA and BECPA are shown with the black solid line and red dashed line, respectively. The probability density displays two peaks near $k = 0$ and $2v_p$. The origin of the second peak is clear if we consider TI in the rest frame of the projectile. In this frame, the initial electron wave packet is scattered on the proton and part of it is reflected back. This reflected part of the wavepacket has velocity $2v_p$ in the laboratory frame. The peak near $k = 0$ is split by the kinematic node at $k = 0$. This node is a characteristic feature for 1D systems with attractive potentials.

The most essential feature of the experimental differential cross sections reported by Schöffler *et al.* [7,8] is the shift of the maximum of the ejected electron momentum distribution in the direction opposite to the projectile motion. In the meantime, the first Born cross sections, reported in the same works, display the main peak which is largely centered around the zero momentum.

It is clearly seen in Fig. 1 that the CPA results demonstrate the same backward shift of the main peak, except for the case of the smallest $v_p = 3$ a.u. The BECPA results demonstrate the forward shift for all v_p. It is easy to explain this behavior by the following qualitative arguments. In the BE process, both the electrons are pushed by projectile, and ionization occurs

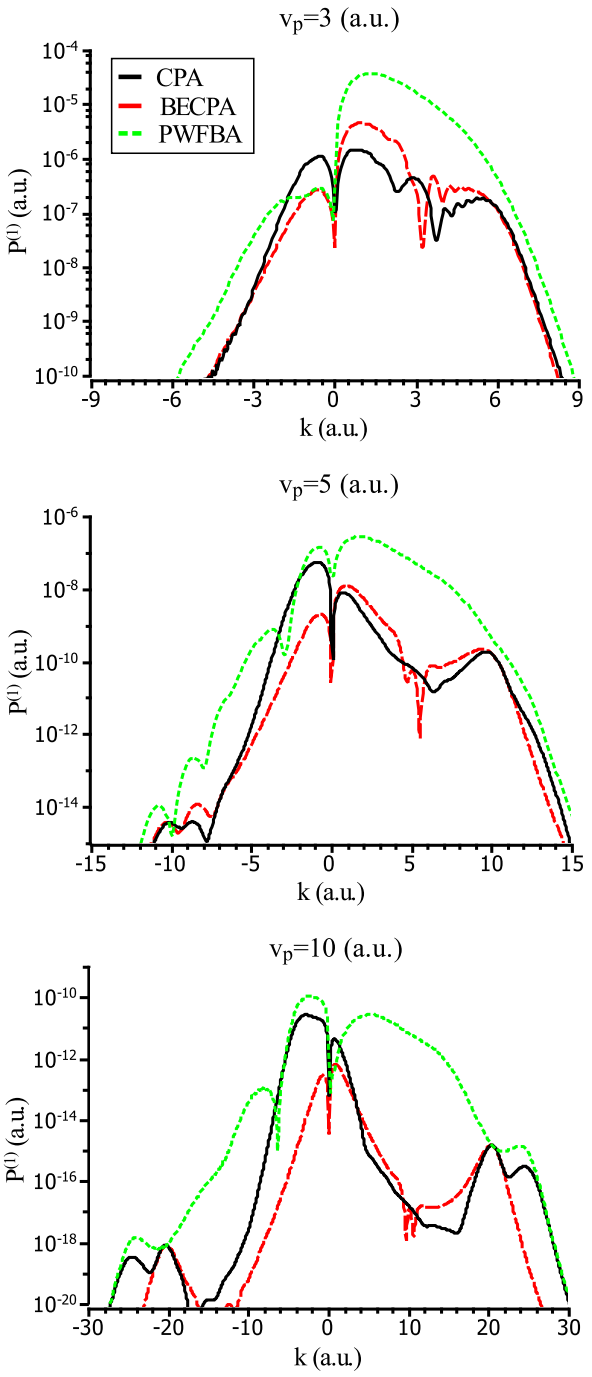

FIG. 1. (Color online) The TI probability density $P^{(1)}(k)$ as a function of the ejected electron momentum for the proton velocities $v_p = 3$ a.u. (top), 5 a.u. (middle), and 10 a.u. (bottom). Various calculations are displayed with the following line styles: the full CPA (black solid line), the BECPA (red dashed line), and the PWFBA (green dotted line).

irrespective of transfer. Since the momentum transferred from the projectile is directed forward, the main peak in the ionization probability is also shifted forward. In the SO process, the second electron is preferably ejected in the direction opposite to the first electron motion which is captured by projectile. The resulting preferable ejection direction depends on the relative weighting of the BE and SO process. Since the SO appears

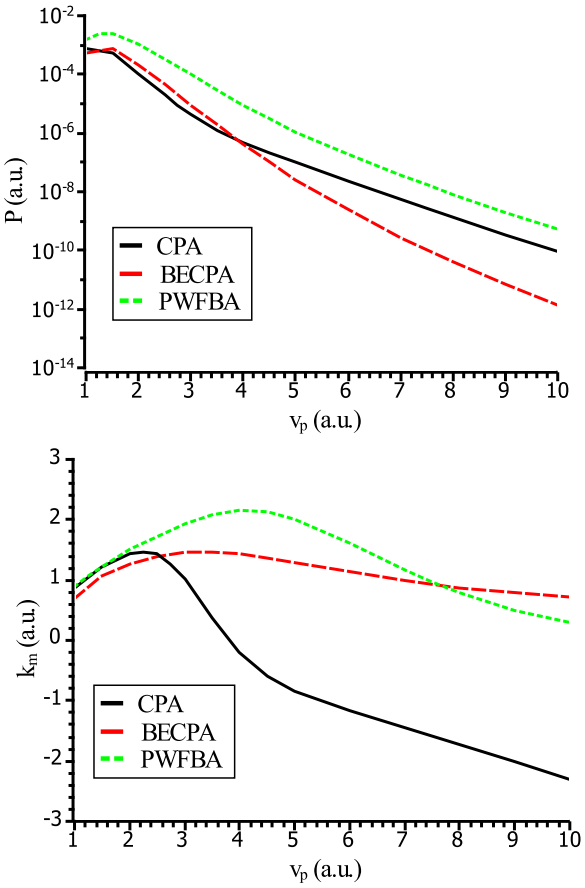

FIG. 2. (Color online) The TI probability P (top) and the mean momentum of ejected electrons $\langle k \rangle$ (bottom) as functions of the projectile velocity v_p. Various calculations are shown as CPA (black solid line), BECPA (red dashed line), and PWFBA (green dotted line).

in the first term of the Born series over the projectile-target interaction, and the BE can only be accommodated by the second and further terms, the SO is dominant at larger v_p, where the ejected electron should be emitted preferentially in the direction opposite to the projectile motion.

To compare the relative contributions of the BE and SO processes and the direction of the preferred emission of the ejected electron depending on v_p, we calculated the total probability of TI and the mean momentum of the ejected electron

$$P = \int_{-\infty}^{\infty} P^{(1)}(k)dk, \tag{24}$$

$$\langle k \rangle = \frac{1}{P}\int_{-\infty}^{\infty} k P^{(1)}(k)dk. \tag{25}$$

By comparing the CPA and BECPA results shown in Fig. 2, it is clearly seen the the BE is dominant at $v_p < 4$ while for larger v_p it is the SO that dominates. In about the same momentum range, the mean momentum $\langle k \rangle$ changes its sign. At larger v_p, the mean momentum becomes large and negative. This indicates that the present CPA results are consistent with the experimental observations. One may suggest that in the first Born approximation (FBA), this preferred backward emission would be even more prominent

feature. However, the plane-wave first Born approximation (PWFBA) [14] strongly overestimates forward emission.

This implies that the deviations of the PWFBA calculations from the experiment [7,8] may be attributed to the shortcomings of this specific implementation.

A. Plane-wave first Born approximation

Let us construct a 1D analog of the PWFBA. In this approximation, the transitional amplitude takes the form

$$A(k) = \langle p_H f|U_1(x_1 - x_p) + U_1(x_2 - x_p) - 2U_1(x_p)|p_p 0\rangle, \tag{26}$$

where the initial-state wave function

$$\langle x_1,x_2,x_p|p_p 0\rangle = \frac{1}{\sqrt{v_p}} e^{ip_p x_p}\varphi_0(x_1,x_2), \tag{27}$$

where $p_p = mv_p$ is the initial proton momentum, m is the proton mass. Following [14], we express the final-state wave function in its asymptotic form

$$\begin{aligned}&\langle x_1,x_2,x_p|p_H f\rangle \\ &= \frac{1}{\sqrt{2v_H}} e^{ip_f x_p}[e^{iv_H x_1}\varphi_{\rm H}(x_1 - x_p)\varphi_k^{(-)}(x_2) \\ &\quad + e^{iv_H x_2}\varphi_{\rm H}(x_2 - x_p)\varphi_k^{(-)}(x_1)].\end{aligned} \tag{28}$$

Here, v_H is the velocity of the neutral hydrogen atom, $p_f = mv_H$ is the proton momentum in the final state. The continuum-state wave functions are normalized by the 1D factors $v_p^{-1/2}$ and $v_H^{-1/2}$. The continuum normalization for various dimensionality is addressed in Ref. [23].

The momentum transfer from the projectile to the target can be expressed as

$$q = p_p - p_f \simeq \frac{1}{v_p}\left[\frac{v_p^2}{2} + \epsilon_{\rm H} + \frac{k^2}{2} - E_0\right]. \tag{29}$$

Similarly to [14], we introduce the momentum difference of the proton projectile and the neutral hydrogen atom

$$Q = p_H - p_p = (m+1)v_H - mv_p = v_H - q. \tag{30}$$

We note that in Ref. [14] this quantity is denoted by q which is reserved in this work to $q = v_H - Q$. Following the cited paper, we split Eq. (26) into the three distinct terms and express them by using the Fourier transform of the functions $\varphi_{\rm H}^*(x - x_p)$ and $U_1(x)$:

$$\begin{aligned}A_1(k) &= \sqrt{2}\iiint_{-\infty}^{+\infty} dx_1 dx_2 dx_p e^{iqx_p - iv_H x_1} \\ &\quad\times \varphi_{\rm H}^*(x_1 - x_p)\varphi_k^{(-)*}(x_2)U_1(x_1 - x_p)\varphi_0(x_1,x_2) \\ &= \int_{-\infty}^{\infty} u_{\rm H}^*(\varkappa)V_1(q - \varkappa)I_k(v_H - q,0)d\varkappa,\end{aligned} \tag{31}$$

$$\begin{aligned}A_2(k) &= \sqrt{2}\iiint_{-\infty}^{+\infty} dx_1 dx_2 dx_p e^{iqx_p - iv_H x_1} \\ &\quad\times \varphi_{\rm H}^*(x_1 - x_p)\varphi_k^{(-)*}(x_2)U_1(x_2 - x_p)\varphi_0(x_1,x_2) \\ &= \int_{-\infty}^{\infty} u_{\rm H}^*(\varkappa)V_1(q-\varkappa)I_k(v_H-\varkappa,-q+\varkappa)d\varkappa,\end{aligned} \tag{32}$$

$$\begin{aligned}A_3(k) &= -2\sqrt{2}\iiint_{-\infty}^{+\infty} dx_1 dx_2 dx_p e^{iqx_p - iv_H x_1} \\ &\quad\times \varphi_{\rm H}^*(x_1 - x_p)\varphi_k^{(-)*}(x_2)U_1(x_p)\varphi_0(x_1,x_2) \\ &= -2\int_{-\infty}^{\infty} u_{\rm H}^*(\varkappa)V_1(q - \varkappa)I_k(v_H - \varkappa,0)d\varkappa.\end{aligned} \tag{33}$$

Here, we introduced the notation

$$\begin{aligned}I_k(\kappa_1,\kappa_2) &= \frac{\sqrt{2}}{(2\pi)^{1/2}}\int_{-\infty}^{\infty}\varphi_k^{(-)*}(x_2)e^{-i\kappa_2 x_2} \\ &\quad\times\left[\int_{-\infty}^{\infty} e^{-i\kappa_1 x_1}\varphi_0(x_1,x_2)dx_1\right]dx_2.\end{aligned} \tag{34}$$

Finally, Eq. (26) takes the form

$$\begin{aligned}A(k) &= \frac{1}{\sqrt{v_p v_H}}\int_{-\infty}^{\infty} d\varkappa\, u_{\rm H}^*(\varkappa)V_1(v_H - Q - \varkappa) \\ &\quad\times[I_k(Q,0) + I_k(v_H - \varkappa,-v_H + Q + \varkappa) \\ &\quad - 2I_k(v_H - \varkappa,0)],\end{aligned} \tag{35}$$

which, apart from notations, coincides with Eq. (2) of Houamer *et al.* [14].

In Fig. 1, we display the probability density calculated with the PWFBA. It is clear that this calculation deviates strongly from the nonperturbative CPA calculation. In the PWFBA, the probability density displays a peak at $k > 0$ which overshoots strongly the CPA peak, both by the magnitude and the width. As is seen on the bottom panel of Fig. 2, this overestimation leads to the mean momentum $\langle k\rangle > 0$ even at large v_p. Hence, the 1D implementation of the PWFBA displays the same characteristic feature as the original implementation used in Refs. [7,8].

In order to elucidate the origin of this behavior, we express the PWFBA amplitude neglecting the interelectron interaction. In this case, $\varphi_0(x_1,x_2) = \varphi_0(x_1)\varphi_0(x_2)$ and

$$\begin{aligned}I_k(\kappa_1,\kappa_2) &= \frac{\sqrt{2}}{(2\pi)^{1/2}}\int_{-\infty}^{\infty}\varphi_k^{(-)*}(x_2)e^{-i\kappa_2 x_2}\varphi_0(x_2)dx_2 \\ &\quad\times\int_{-\infty}^{\infty} e^{-i\kappa_1 x_1}\varphi_0(x_1)dx_1 \\ &= \sqrt{2}u_0(\kappa_1)I_k(\kappa_2),\end{aligned}$$

where

$$I_k(\kappa) = \int_{-\infty}^{\infty}\varphi_k^{(-)*}(x)e^{-i\kappa x}\varphi_0(x)dx.$$

Then, Eq. (36) takes the form

$$\begin{aligned}A(k) &= \frac{\sqrt{2}}{\sqrt{v_p v_H}}\int_{-\infty}^{\infty} u_{\rm H}^*(\varkappa - v_H)V_1(\varkappa - Q) \\ &\quad\times[u_0(Q)I_k(0) + u_0(\varkappa)I_k(Q - \varkappa) - 2u_0(\varkappa)I_k(0)]d\varkappa.\end{aligned}$$

Since $I_k(0) = 0$, the only second term survives under the integral sign, i.e.,

$$\begin{aligned}A(k) &= A_2(k) \\ &= \frac{\sqrt{2}}{\sqrt{v_p v_H}}\int_{-\infty}^{\infty} u_{\rm H}^*(\varkappa - v_H)V_1(\varkappa - Q)I_k(Q-\varkappa)u_0(\varkappa)d\varkappa.\end{aligned}$$

The authors of Refs. [7,8,14] claim that this term is responsible for the BE process. However, BE should be zero in the FBA. The projectile can only act on one of the target electrons and the second electron makes no transition in the absence of the interelectron interaction. The reason why the term A_2 is not zero becomes clear if we write it in its original form as the coordinate integral

$$A_2(k) = \sqrt{2}\int_{-\infty}^{\infty} dx_p e^{iqx_p} \int_{-\infty}^{\infty} dx_1 e^{-iv_H x_1} \varphi_{\rm H}^*(x_1 - x_p)\varphi_0(x_1) \times \int_{-\infty}^{\infty} \varphi_k^{(-)*}(x_2) U_1(x_2 - x_p)\varphi_0(x_2) dx_2.$$

One can see that the projectile interaction causes ionization (the integral over x_2) and the transfer takes place due to the nonorthogonality of the initial- and final-state wave functions

$$\langle \varphi_0(x)|\, e^{iv_H x}\varphi_{\rm H}(x - x_p)\rangle \neq 0.$$

Thus A_2 is the artifact of the approximation employed in [7,8,14].

Note that the term A_3 appears due to proton-nucleus interaction. In CPA, the proton-nucleus potential only adds an overall time-dependent phase factor to the wave function, and thus is unable to produce change of the electronic state. In the Jackson-Schiff (JS) theory of a related process of simple transfer, an introduction of the proton-nucleus potential compensates a spurious term appearing due to the nonorthogonality of the initial and final states [24,25]. For transfer ionization, A_3 plays an analogous role, but it does not provide the full compensation.

It is possible to eliminate the spurious electron transfer by orthogonalizing the single-particle initial and captured electron states. For this purpose, in Eqs. (31), (32), and (33) one shall replace $\varphi_0(x_1,x_2)$ by

$$\tilde{\varphi}_0(x_1,x_2,x_p) \equiv \varphi_0(x_1,x_2) - \langle e^{iv_H x_1}\varphi_{\rm H}(x_1 - x_p)|\varphi_0(x_1,x_2)\rangle \times e^{iv_H x_1}\varphi_{\rm H}(x_1 - x_p). \quad (36)$$

It is easy to see that $A_2 \equiv 0$ and $A_3 \equiv 0$ after this replacement. However, this operation does not assure that A_1 gives the correct result.

B. Other theoretical models of TI in 1D

For further insight, we examine pure ionization and pure transfer separately for single electron. The FBA amplitude of ionization can be expressed as

$$A_{\rm SI1B}(k) = \langle p_f k|U_1(x - x_p)|p_p 0\rangle = \frac{1}{\sqrt{v_p v_f}}\langle k|\exp(iqx)|0\rangle V_1(q) = \frac{1}{\sqrt{v_p v_f}} V_1(q) I_k(-q), \quad (37)$$

where the momentum transfer is $q = p_p - p_f \simeq (k^2/2 - \epsilon_0)/v_p$ and the initial- and final-state wave functions take the form

$$\langle x,x_p|p_p 0\rangle = \frac{1}{\sqrt{v_p}} e^{ip_p x_p}\varphi_0(x); \quad (38)$$

$$\langle x,x_p|p_f k\rangle = \frac{1}{\sqrt{v_f}} e^{ip_f x_p}\varphi_k^{(-)}(x). \quad (39)$$

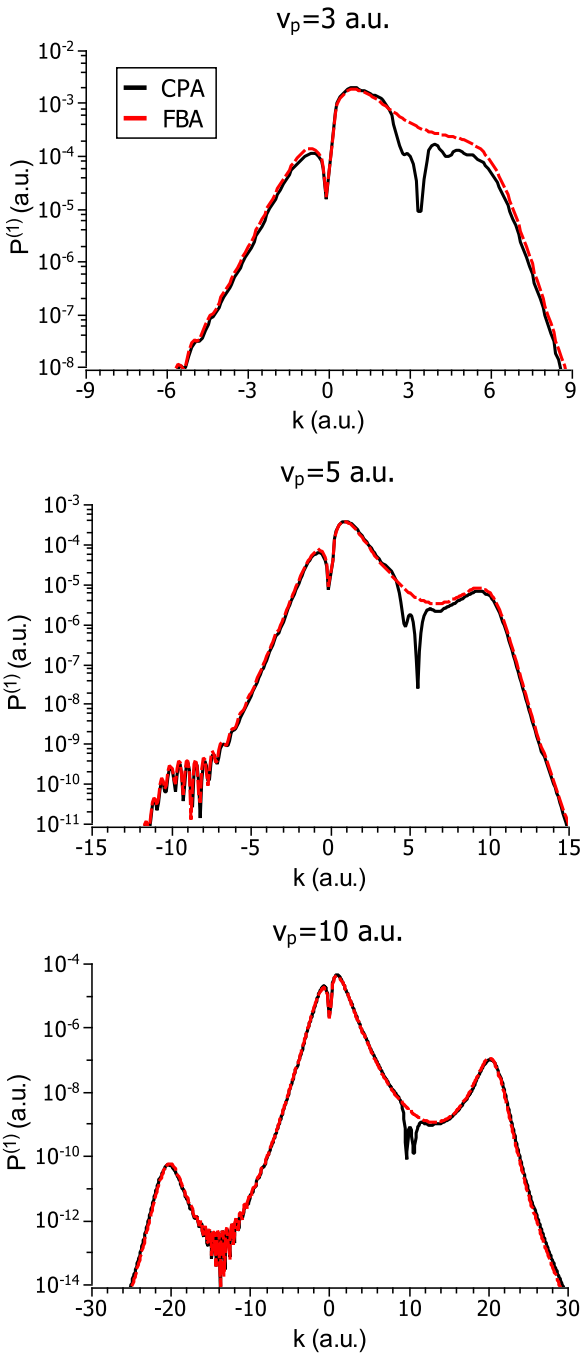

FIG. 3. (Color online) Ionization probability density $P^{(1)}(k)$ as a function of the momentum of the ejected electron for the proton velocities $v_p = 3$ a.u. (top), 5 a.u. (middle), and 10 a.u. (bottom). The following calculations are shown: CPA (black solid line) and FBA (red dashed line).

One can see from Fig. 3 that the FBA and CPA results are quite close except for the electron momenta $k \approx v_p$ where the FBA overshoots CPA rather strongly. For these momenta, the electrons are captured by the protons quite efficiently which is not accounted by FBA.

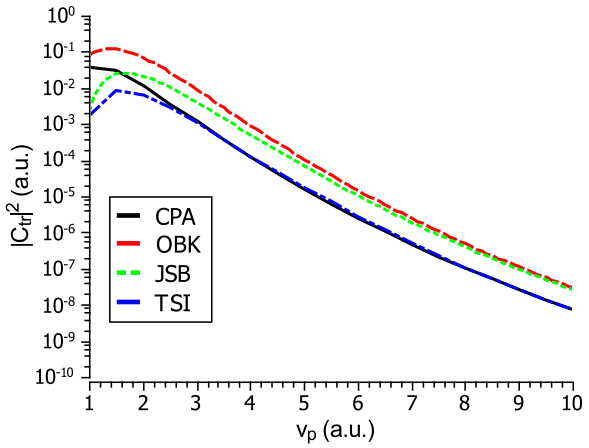

FIG. 4. (Color online) Transfer probability as a function of the proton velocity v_p: CPA (black solid line), OBK (red dashed line), JSB (green dotted line), TSI (blue dotted-dashed line).

Now let us consider capture. The OBK amplitude in 1D kinematics has the form

$$C_{\rm OBK} = \langle p_f f|U_1(x-x_p)|p_p 0\rangle = \frac{1}{\sqrt{v_p v_H}} u_0(v_H - q)\int_{-\infty}^{\infty} u_{\rm H}^*(\eta - q)V_1(\eta)d\eta, \quad (40)$$

where the momentum transfer $q \simeq (v_p^2/2 + \epsilon_{\rm H} - \epsilon_0)/v_p$, and the final-state wave function describes the hydrogen atom flying away with the velocity v_H:

$$\langle x,x_p|p_H f\rangle = \frac{1}{\sqrt{v_H}} e^{ip_f x_p + iv_H x}\varphi_{\rm H}(x-x_p). \quad (41)$$

It is seen from Fig. 4 that the OBK overshoots CPA quite considerably. Now let us check if we can improve the OBK result by a simple orthogonalization of the initial- and final-state wave functions

$$\langle x,x_p|f_O\rangle = e^{iv_H x}\varphi_{\rm H}(x-x_p) - \langle\varphi_0(x)|\, e^{iv_H x}\varphi_{\rm H}(x-x_p)\rangle\varphi_0(x). \quad (42)$$

It is easy to show that the orthogonalization is equivalent to the OBK formula with the original nonorthogonalized wave functions modified by a perturbation potential

$$C_{\rm JSB} = \langle p_f f|U_1(x-x_p) - \bar{U}_1(x_p)|p_p 0\rangle, \quad (43)$$

where the balancing potential

$$\bar{U}_1(x_p) = \langle 0|U_1(x-x_p)|0\rangle. \quad (44)$$

The balancing potential $\bar{U}_1(x_p) \approx U_1(x_p)$, where $-U_1(x_p)$ can be considered as proton-nucleus potential. Hence, for transfer from the neutral hydrogen, Eq. (43) is close to the JS approximation. Here, we consider transfer from the helium ion, and a formal application of the JS approximation for this case gives a perturbation potential $U_1(x-x_p) - U_2(x_p)$. But, Bates [24,25] and, lately, Lin *et al.* [26] have shown that advantage of JS over OBK lie in the fact that the nuclear potential compensates a spurious term from the nonorthogonality of the initial-and final-state functions. The balancing potential should be used instead of the nuclear potential in a general case [26]. For these reasons, the approach given by Eq. (43) can be considered as an improved JS approximation, and we named it as Jackson-Schiff-Bates (JSB) approximation. It is clear from Fig. 4 that the OBK and JSB results differ only at small v_p, but at large v_p both calculations significantly overshoot the CPA.

Now, let us tackle the problem from another side. Suppose that an ionization takes place and the ejected electron is then captured whose momentum distribution coincides with the momentum-space components of the electron bound to the proton. In this case, the transfer amplitude will be equal to the overlap integral

$$C_{\rm trSI} = \int_{-\infty}^{\infty} u_{\rm H}^*(k - v_H)A_{\rm SI1B}(k)dk. \quad (45)$$

We call this approach the transfer via single ionization (TSI) in the first Born approximation. By inspecting Fig. 4, one can conclude that the TSI and CPA results are practically coincident at large v_p.

In the time-dependent formalism, the TSI is equivalent to solving the following TDSE:

$$i\frac{\partial\psi_1(x,t)}{\partial t} = \hat{h}_0\psi_1(x,t) + U_1(x - v_p t)\varphi_0(x)e^{-i\epsilon_0 t} \quad (46)$$

and subsequent projection of the solution $\psi_1(x,t)$ to the function

$$\tilde{\psi}_{\rm tr}(x,t) = \int_{-\infty}^{\infty} u_{\rm H}(k - v_H)\varphi_k^{(-)}(x)\exp\left(-i\frac{k^2}{2}t\right)dk \quad (47)$$

instead of the function (13). Since the proton potential in Eq. (46) acts solely as a perturbation, the bound state of the proton and electron cannot be described by this equation. The function (47) describes the outgoing wavepacket, but unlike Eq. (13) it is a solution of Eq. (46) at $t \to \infty$. More broadly, the major difference of TSI and OBK/JS is that the Born matrix element is calculated in the former between the eigenfunctions of the same Hamiltonian $\hat{h}_0$, whereas in the latter these functions belong to different Hamiltonians.

C. Transfer ionization via double ionization

Similar to TSI for simple transfer, we develop a method to calculate TI via double ionization (TIDI). The double-ionization amplitude in the FBA has the form

$$A_{\rm DI1B}(k_1,k_2) = \langle p_f k_1 k_2|U_1(x_1 - x_p) + U_1(x_2 - x_p)|p_p 0\rangle, \quad (48)$$

where the initial- and final-state wave functions

$$\langle x_1,x_2,x_p|p_p 0\rangle = \frac{1}{\sqrt{v_p}} e^{ip_p x_p}\varphi_0(x_1,x_2); \quad (49)$$

$$\langle x_1,x_2,x_p|p_f k_1 k_2\rangle = \frac{1}{\sqrt{v_f}} e^{ip_f x_p}\varphi_{k_1 k_2}^{(-)}(x_1,x_2). \quad (50)$$

After integration over x_p we obtain

$$A_{\rm DI1B}(k_1,k_2) = \frac{1}{\sqrt{v_p v_f}}\langle k_1 k_2|\exp(iqx_1) + \exp(iqx_2)|0\rangle V_1(q), \quad (51)$$

where the momentum transfer

$$q = p_p - p_f \simeq \frac{1}{v_p}\left(\frac{k_1^2}{2} + \frac{k_2^2}{2} - E_0\right). \quad (52)$$

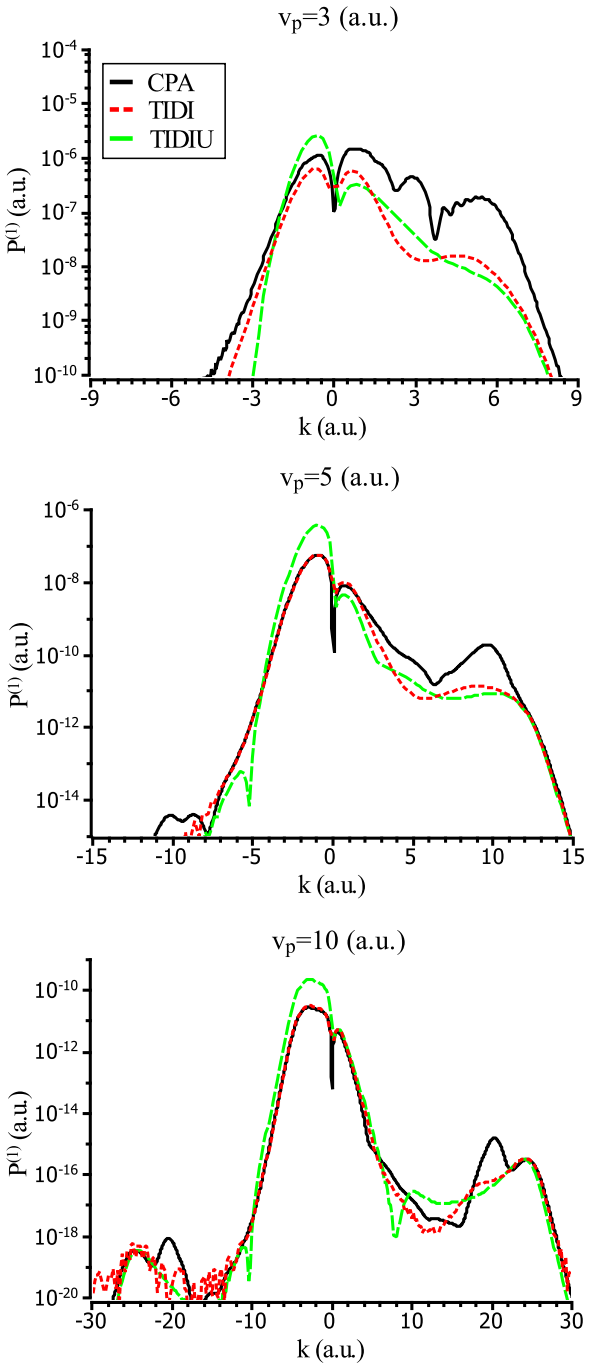

FIG. 5. (Color online) TI probability density $P^{(1)}(k)$ as a function of the momentum of the transferred electron for the proton velocities $v_p = 3$ a.u. (top), 5 a.u. (middle), and 10 a.u. (bottom). Various calculations are shown as CPA (black solid line), TIDI (red dotted line), TIDIU (green dashed line).

The TI amplitude is calculated as

$$A_{\mathrm{trDI}}(k) = \sqrt{2}\int_{-\infty}^{\infty} u_{\mathrm{H}}^{*}(k_1 - v_H)A_{\mathrm{DI1B}}(k_1,k)dk_1. \quad (53)$$

From Fig. 5 it is obvious that at large v_p and small k the TIDI and CPA results are practically coincident. And from Fig. 6 it is clear that both the total TI probability P and the mean elected electron momentum $\langle k\rangle$, are also very close between

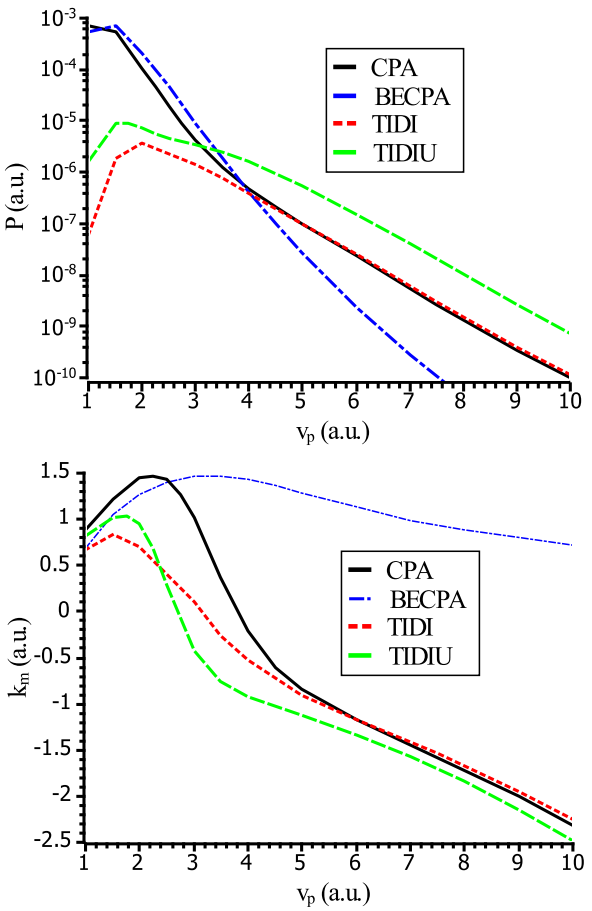

FIG. 6. (Color online) The total TI probability P (top) and the mean momentum of ejected electron $\langle k\rangle$ (bottom) as functions of v_p. Various calculations are shown as CPA (black solid line), TIDI (red dotted line), TIDIU (green dashed line), BECPA (blue dashed-dotted line).

the TIDI and CPA in the whole region of dominance of the SO. On the top panel of Fig. 6, the crossover between the BE and SO mechanisms is seen most graphically: at $v_p < 4$ the CPA curves is close to that of the BECPA, whereas at $v_p > 4$ to that of the TIDI.

From Fig. 5 one can observe that for large k, the difference between TIDI and CPA is much more prominent. This is explained by a large contribution of the BE process to TI at large k even at large v_p. By comparing the bottom panels of Figs. 1 and 5, one can discern some interesting details explaining the origin of a double peak near $k = 2v_p$. As we mentioned before, this peak appears due to the reflection of the ejected electrons by the proton potential. It is clearly seen on the bottom panel of Fig. 1 the first half of this peak (at lower momenta) is due to the BE process, and from the bottom panel of Fig. 5 it is clear that the second half (at larger momenta) is due to the SO. In the latter case, the sequence events giving rise to TI are the following. First, the impinging proton reflects the electron which flies away with the velocity $k = 2v_p$, then the second electron, emitted due to the SO, is captured by the proton.

In 3D kinematics, TI can proceed via the nuclear or electron Thomas processes [27]. In these processes, the electron

scattered by the proton acquires a velocity v_p or $\sqrt{2}v_p$ and, then, in the secondary scattering from, respectively, the nucleus or the second electron, receives a velocity $\mathbf{v}_p$ to be captured by the proton. The Thomas processes are not possible in 1D kinematics because the electron scattered on the proton acquires either zero or $2v_p$ velocity in this case.

To pinpoint the role of interelectron interaction in the final state, we also performed calculations with uncorrelated wave functions of the two-electron continuum orthogonalized to the initial state

$$\tilde{\varphi}^{(-)}_{k_1k_2}(x_1,x_2) = \chi^{(-)}_{k_1k_2}(x_1,x_2) - \left\langle \chi^{(-)}_{k_1k_2}|0\right\rangle \varphi_0(x_1,x_2), \quad (54)$$

where

$$\chi^{(-)}_{k_1k_2}(x_1,x_2) = \frac{1}{\sqrt{2}}\left[\varphi^{(-)}_{k_1}(x_1)\varphi^{(-)}_{k_2}(x_2) + \varphi^{(-)}_{k_2}(x_1)\varphi^{(-)}_{k_1}(x_2)\right]. \quad (55)$$

This approximation is labeled as TIDIU.

From Fig. 6, it is clear that the TIDIU overestimates significantly the value of P. The mean momentum $\langle k\rangle$ is rather close to the exact solution, only slightly overestimated in the negative region. It is seen in Fig. 5 that overestimated P is due to a strong growth of the peak at small $k < 0$, whereas at small $k > 0$ the TIDIU calculation is close to both the TIDI and CPA. Thus, we can conclude that the interelectron correlation in the final state suppresses partially the backward emission and works out of sync with the correlation in the initial state.

IV. CONCLUSION

We have performed time-dependent calculations of transfer ionization in the fast proton scattering on the helium atom. We solved a time-dependent Schrödinger equation under the classical projectile motion approximation in one-dimensional kinematics. To gain deeper physical insight into specific mechanisms of the TI reaction, we also performed various perturbative 1D calculations which mimicked realistic first Born calculations performed by other authors. We identified a strong effect of the nonorthogonality of the initial and final states which may lead to some spurious unphysical terms. This term may be responsible for poor performance of the FBA employed by other authors.

Among various approximate perturbative TI schemes, the most accurate calculation is obtained by overlapping the double-ionization amplitude with the momentum profile of the final-state wave function. This indicates that the most probable scenario of TI involves double ionization and subsequent capture of those of the ionized electrons which fall into the attractive potential well of the proton by matching its velocity.

Because both Godunov *et al.* [9,12,13] and Popov *et al.* [7,8,14] employ a very similar formalism based on the Jackson-Schiff approximation, our remarks on possible flaws of the FBA concern both groups of authors. But, of course, our conclusions can only be verified after a full 3D CPA and TIDI calculations are performed and satisfactory agreement with experiment is achieved. More broad is the question of using nonorthogonal initial and final states belonging to different Hamiltonians in perturbative calculations. This question goes beyond the scope of this work. The same question was a matter of discussion in theory of simple transfer much earlier [24–26,28].

In the future, we intend to extend our 1D model to full dimensionality under the same classical projectile motion approximation.

ACKNOWLEDGMENTS

We acknowledge M. Schöffler and R. Dörner for critical reading of the manuscript and Y. Popov for useful and stimulating discussions. V.V.S. acknowledges support from the Russian Foundation for Basic Research (Grant No. 14-01-00420-a).

[1] E. Horsdal, B. Jensen, and K. O. Nielsen, Phys. Rev. Lett. **57**, 1414 (1986).
[2] J. Pálinkás, R. Schuch, H. Cederquist, and O. Gustafsson, Phys. Rev. Lett. **63**, 2464 (1989).
[3] V. Mergel, R. Dörner, K. Khayyat, M. Achler, T. Weber, O. Jagutzki, H. J. Lüdde, C. L. Cocke, and H. Schmidt-Böcking, Phys. Rev. Lett. **86**, 2257 (2001).
[4] H. Schmidt-Böcking, V. Mergel, R. Dörner, C. L. Cocke, O. Jagutzki, L. Schmidt, T. Weber, H. J. Ludde, E. Weigold, Y. V. Popov *et al.*, Europhys. Lett. **62**, 477 (2003).
[5] H. Schmidt-Böking, V. Mergel, R. Dörner, H. J. Lüdde, L. Schmidt, T. Weber, E. Weigold, and A. S. Kheifets, *Many-Particle Quantum Dynamics in Atomic and Molecular Fragmentation* (Springer, Heidelberg, 2003), pp. 353–378.
[6] H. T. Schmidt, J. Jensen, P. Reinhed, R. Schuch, K. Støchkel, H. Zettergren, H. Cederquist, L. Bagge, H. Danared, A. Källberg *et al.*, Phys. Rev. A **72**, 012713 (2005).
[7] M. S. Schöffler, O. Chuluunbaatar, Y. V. Popov, S. Houamer, J. Titze, T. Jahnke, L. P. H. Schmidt, O. Jagutzki, A. G. Galstyan, and A. A. Gusev, Phys. Rev. A **87**, 032715 (2013).
[8] M. S. Schöffler, O. Chuluunbaatar, S. Houamer, A. Galstyan, J. N. Titze, L. P. H. Schmidt, T. Jahnke, H. Schmidt-Böcking, R. Dörner, Y. V. Popov *et al.*, Phys. Rev. A **88**, 042710 (2013).
[9] A. L. Godunov, C. T. Whelan, H. R. J. Walters, V. S. Schipakov, M. Schöffler, V. Mergel, R. Dörner, O. Jagutzki, L. P. H. Schmidt, J. Titze *et al.*, Phys. Rev. A **71**, 052712 (2005).
[10] M. Schulz, X. Wang, M. Gundmundsson, K. Schneider, A. Kelkar, A. B. Voitkiv, B. Najjari, M. Schöffler, L. P. H. Schmidt, R. Dörner *et al.*, Phys. Rev. Lett. **108**, 043202 (2012).
[11] K. Schneider, M. Schulz, X. Wang, A. Kelkar, M. Grieser, C. Krantz, J. Ullrich, R. Moshammer, and D. Fischer, Phys. Rev. Lett. **110**, 113201 (2013).
[12] A. L. Godunov, C. T. Whelan, and H. R. J. Walters, J. Phys. B: At., Mol. Opt. Phys. **37**, L201 (2004).
[13] A. L. Godunov, C. T. Whelan, and H. R. J. Walters, Phys. Rev. A **78**, 012714 (2008).
[14] S. Houamer, Y. V. Popov, and C. Dal Cappello, Phys. Rev. A **81**, 032703 (2010).
[15] A. S. Kheifets, I. Bray, and K. Bartschat, J. Phys. B: At., Mol. Opt. Phys. **32**, L433 (1999).

[16] A. B. Voitkiv, B. Najjari, and J. Ullrich, Phys. Rev. Lett. **101**, 223201 (2008).
[17] A. B. Voitkiv, J. Phys. B: At., Mol. Opt. Phys. **41**, 195201 (2008).
[18] A. B. Voitkiv and X. Ma, Phys. Rev. A **86**, 012709 (2012).
[19] Y. V. Popov, V. L. Shablov, K. A. Kouzakov, and A. G. Galstyan, Phys. Rev. A **89**, 036701 (2014).
[20] A. B. Voitkiv and X. Ma, Phys. Rev. A **89**, 036702 (2014).
[21] J. H. McGuire, *Electron Correlation Dynamics in Atomic Collisions*, Cambridge Monographs on Atomic, Molecular and Chemical Physics (Cambridge University Press, Cambridge, 1997).
[22] V. V. Serov, V. L. Derbov, T. A. Sergeeva, and S. I. Vinitsky, Phys. Rev. A **88**, 043403 (2013).
[23] L. D. Landau and E. M. Lifshitz, *Quantum Mechanics (Non-relativistic theory)*, 3rd ed., Vol. 3 of Course of Theoretical Physics (Pergamon, Oxford, 1985).
[24] D. R. Bates and A. Dalgarno, Proc. Phys. Soc. A **65**, 919 (1952).
[25] D. R. Bates, Proc. R. Soc. London, Ser. A **247**, 294 (1958).
[26] C. D. Lin, S. C. Soong, and L. N. Tunnell, Phys. Rev. A **17**, 1646 (1978).
[27] J. S. Briggs and K. Taulbjerg, J. Phys. B: At. Mol. Phys. **12**, 2565 (1979).
[28] C. D. Lin, J. Phys. B: At. Mol. Phys. **11**, L185 (1978).